Simulation of Sedimentation of Polydisperse Suspensions: A Particle-Based Approach

Monika Bargieł
Institute of Computer Science, AGH University of Science and Technology, al. Mickiewicza 30, 30-059 Cracow, Poland

Robert A. Ford
Spielo Gaming International, 328 Urquhart Ave., Moncton, NB, E1H 2R6, Canada

Elmer M. Tory
Dept. of Mathematics and Computer Science, Mount Allison University, Sackville, NB, E4L 1G6, Canada

DOI 10.1002/aic.10517
Published online June 24, 2005 in Wiley InterScience (www.interscience.wiley.com).

The global behavior of sedimenting monodisperse suspensions of rigid spheres can be deduced from the flux plot, but this approach is not available for polydisperse suspensions. The rapid increase in computing power has made simulation an attractive method. Sedimentation of suspensions with many species can now be handled easily. Two sources of difficulty, generation of a concentration gradient and control of fluctuations in concentration, can be overcome by choosing the controlling concentration as that immediately below the test sphere. Applied to randomly distributed particles, our deterministic algorithm yields the ensemble behavior of each species and prepares the way for stochastic simulations by correcting density inversions. The simplicity and generality of the method make it feasible to test any theoretical or empirical model against any experimental data. Simulating the experiments and comparing the simulated and experimental results is illustrated. © 2005 American Institute of Chemical Engineers *AIChE J,* 51: 2457–2468, 2005
Keywords: simulation, settling, sedimentation, polydisperse suspensions

Introduction

Particles in industrial polydisperse suspensions have a wide variety of shapes and sizes. Though there has been some progress in treating the sedimentation of nonspherical particles,[1,2] many theoretical and experimental studies have dealt with rigid spheres. Most of the early and many of the later articles reported results for monodisperse suspensions.[3,4] Despite the attention paid to these, polydisperse suspensions are far more common. Some spheres are so nearly uniform that they are essentially identical.[5,6,7] However, many experiments with "monodisperse" suspensions involve spheres that have an approximately normal distribution with a considerable spread in diameters.[8,9] Similarly, each species in a "bidisperse" or "tridisperse" suspension often has a distribution of diameters.[10] Suspensions with a wide variation in size are also common.[11]

There are several model equations that predict initial settling rates in polydisperse suspensions,[4,12] but only recently have sophisticated numerical methods been used to predict the complete behavior of a sedimenting suspension.[13] We simulate the settling paths of the individual particles in a suspension and thereby obtain the global behavior. This alternative approach reproduces all the qualitative features of one-dimensional (1-D) sedimentation, and facilitates quantitative tests of model equations.

Theory

The sedimentation process

We consider the sedimentation of a polydisperse suspension of rigid spheres. Let $\mathbf{\Phi} = (\phi_1, \phi_2, \ldots, \phi_K)^T$ be the vector of

Correspondence concerning this article should be addressed to M. Bargieł at mbargiel@uci.agh.edu.pl.

solids concentrations (volume fractions) of K species, and $\phi = \phi_1 + \phi_2 + \cdots + \phi_K$ be the total solids concentration. Then, sedimentation is the evolution of $\mathbf{\Phi}(z, t)$, $0 < z \leq H$, $t \geq 0$, from $\mathbf{\Phi}_0$ to $\mathbf{\Phi}_{\max}(z)$ where $\mathbf{\Phi}_0$ is the initial value of $\mathbf{\Phi}$ and $\mathbf{\Phi}_{\max}$ is the value when $\phi = \phi_{\max}$, the maximum total solids concentration attained in the polydisperse system. (For simplicity, we ignore any variation in $\phi_{\max}$ with z.) This evolution is governed by the solids flux vector $\mathbf{f} = (f_1, f_2, \ldots, f_K)$, where $f_k = \phi_k v_k$. The two essentials for predicting this evolution are a model equation (a means of predicting settling velocities from solids concentrations, that is, $v_k(\mathbf{\Phi})$, $k = 1, \ldots, K$), and a method of implementing the changes produced by the flux. The global behavior of sedimenting monodisperse suspensions can be deduced from the flux plot,[3, 14, 15, 16] but this approach is not available for polydisperse suspensions. For these, the settling process depends not only on the total flux $f = f_1 + f_2 + \cdots + f_K$, but also on the components f_k.

Experimentally, the three principal features of the behavior of polydisperse suspensions are segregation of species by size and/or density, propagation of concentration gradients under certain conditions, and correction of density inversions by the ensemble movements of groups of particles. Sophisticated numerical methods can detect and preserve the discontinuities in concentration that theoretically occur in these suspensions.[11, 13] In practice, interface broadening by hydrodynamic diffusion modifies these discontinuities to sharp or even gradual changes.[9]

An alternative approach is to simulate the behavior of the individual particles in a suspension,[17] and thereby obtain the global behavior.[18, 19, 20, 21, 22] Unlike these previous studies, ours makes the velocity of a particle dependent on the concentration of the region immediately below. This allows simulations to reproduce the features of real suspensions, including the propagation of concentration gradients and the smoothing of fluctuations.

Model equations for monodisperse suspensions

There are many empirical or semiempirical equations, such as those of Steinour,[23] Richardson and Zaki,[24] and Barnea and Mizrahi, [25] for the velocity $v(\phi)$ of a monodisperse suspension. Of these, the best known and most widely used is the Richardson-Zaki equation

$$v(\phi) = u_\infty (1 - \phi)^n \tag{1}$$

where u_∞ is the Stokes velocity

$$u_\infty = -\Delta\rho g d^2/(18\eta_f) \tag{2}$$

Here $\Delta\rho$ is the solid-fluid density difference, g the acceleration of gravity, d the diameter of the sphere, and η_f the dynamic viscosity of the fluid. Until higher concentrations are propagated upwards from the base of the container, the solids concentration in the upper region usually remains approximately constant at its initial value. Then, the velocity of the spheres in the region just below the slurry-fluid interface is also the interface velocity, and measuring it yields $v(\phi)$. (Tory and Pickard,[5, 18] Tory et al.[26] and Bürger and Tory[16] cite experimental evidence that, when the sphere-cylinder diameter ratio is very small, particles near the interface settle more slowly than those in the bulk of a dilute suspension.[27] We do not consider this case.)

Since identical spheres at the same concentration typically have different velocities,[7, 28] $v(\phi)$ is actually a mean velocity. The variability of velocities about this mean can be expressed as a stochastic component[5, 17, 19, 28] that leads to hydrodynamic diffusion.[29] In this article, we consider only a deterministic dependence of velocity on concentration.

Simulation of monodisperse suspensions

When solids concentration varies with height, we need to specify the concentration, ϕ^i, that applies to the ith sphere. (All terms referencing the ith sphere are designated by a superscript i to distinguish them from terms referencing species, which are designated by subscripts, for example, ϕ_k). Using the Richardson-Zaki equation, we write

$$v^i(\phi^i) = \begin{cases} u_\infty (1 - \phi^i)^n, & 0 \leq \phi^i < \phi_{\max} \\ 0, & \text{otherwise.} \end{cases} \tag{3}$$

Beenakker and Mazur[30] calculated the mean velocity of a test sphere in a dilute suspension of identical spheres, settling toward an infinite horizontal flat plate and showed that only spheres in small interval of height affected that velocity. However, spheres in an interval close to the plate settled more slowly than those further away. In our particle-based simulation, the velocity of each particle is governed by the solids concentration in a thin region (of height h) immediately below that particle. The thickness, h, must be large enough to measure concentration accurately, but small enough to emphasize the concentration near the test particle. If the number of particles is very large, this region can be quite thin. However, it must be thick enough to ensure that the test sphere stays in the region throughout the time step. To handle the lowest particles, we set $\phi = \phi_{\max}$ in an artificial region (of thickness h) below the bottom.[3] The particles in this region are uniformly distributed over h.

This specification of the governing concentration has several advantages. It ensures that the particles at the top of a uniformly mixed suspension initially settle with the same velocity as those below. This corresponds to the usual idea of the dependence of interface velocity. It also incorporates the fact that a particle approaching a flat plate or a fixed bed slows down.[2, 31, 32, 33] Finally, it recognizes that a dense region above a dilute one settles rapidly into or through the latter.[5, 34] Choosing the velocity-determining region as that directly below the test sphere maximizes the retarding effect of the packed bed. However, this effect is not directly comparable to that of lubrication terms.[2] In particular, spheres in our simulation settle into the bed with a finite velocity; this keeps the computation time at a reasonable value.

This scheme works as follows: The particles are initially distributed uniformly or randomly over the total height of the column. In the first time-step, all particles above h have the same velocity, but those below settle more slowly because they are affected by particles in the artificial sublayer. The lowest particle is in the region where the effective concentration is the greatest, so it will settle the slowest. The next lowest particle will settle slightly faster, and so on. Each step increases the

concentration in $(0, h)$. If the timestep is sufficiently small, this soon produces a concentration gradient ranging from $\phi_{\max}$ at the bottom to ϕ_0. This is more realistic than Kynch's assumption that these concentrations form immediately.[15]

Model equations for polydisperse suspensions

The appropriate generalization of the Richardson-Zaki equation to K species is the Masliyah-Lockett-Bassoon (MLB) equation[12, 35, 36]

$$v_k = \mu(1-\phi)^{n-2}\Big[\delta_k(\rho_k - \rho(\mathbf{\Phi})) - \sum_{j=1}^{K}\delta_j\phi_j(\rho_j - \rho(\mathbf{\Phi}))\Big], \quad k = 1, \ldots, K \quad (4)$$

where

$$\rho(\mathbf{\Phi}) = \rho_f(1-\phi) + \rho_1\phi_1 + \rho_2\phi_2 + \cdots + \rho_K\phi_K \quad (5)$$

$$\delta_k = d_k^2/d_1^2, \quad \mu = -gd_1^2/(18\eta_f) = u_{\infty 1}/(\rho_1 - \rho_f) \quad (6)$$

ρ_k is the density, and d_k the diameter of spheres of the kth-largest species, ρ_f is the density of the fluid, and $u_{\infty 1}$ is the Stokes velocity of the largest species. Note that $u_{\infty 1} < 0$ when $\rho_1 - \rho_f > 0$.

The fundamental assumption in the rigorous derivation[12, 37] of the MLB equation is that the solid-fluid interaction force between the ith species and the fluid is given by a concentration-dependent factor multiplying the slip velocity, or solid-fluid relative velocity $v_k - v_f$. This approach is consistent with the principle that constitutive equations should be stated in terms of objective quantities. It is well known that the difference between two velocities is objective, while a single velocity is not.[38] Inserting this assumption into the reduced momentum balances for each solids species and the fluid, and choosing a Richardson-Zaki dependence, viz.

$$V(\mathbf{\Phi}) = \begin{cases} (1-\phi)^{n-2}, & 0 \le \phi < \phi_{\max} \\ 0, & \text{otherwise} \end{cases} \quad (7)$$

we obtain Eq. 4.

When $\rho_1 = \rho_2 = \cdots = \rho_K$, this reduces to

$$v_k^i(\mathbf{\Phi}^i) = u_{\infty 1}(1-\phi^i)^{n-1}[\delta_k - (\delta_1\phi_1^i + \cdots + \delta_K\phi_K^i)], \quad k = 1, \ldots, K \quad (8)$$

as the velocity of the ith sphere of the kth species.[37] The concentration vector, $\mathbf{\Phi}^i = (\phi_1^i, \phi_2^i, \ldots, \phi_K^i)^T$, determines that velocity. Here ϕ_j^i is the concentration of the jth species in the region that applies to the ith sphere. Equation 8 clearly reduces to Eq. 1, when only a single species is present. Thus, Equations 1, 8 and 4 constitute a consistent, unified approach to the sedimentation of rigid spheres.

We say that $\mathbf{\Phi} < \mathbf{\Phi}^*$ if $\phi_j < \phi_j^*$ and $\phi_k \le \phi_k^*$, $k \ne j$. It is easily shown that $\partial v_k(\mathbf{\Phi})/\partial\phi_j > 0$ when $v_k(\mathbf{\Phi}) < 0$. (Recall that downward velocities are negative.) Then $\mathbf{\Phi} < \mathbf{\Phi}^*$ implies that $v_k(\mathbf{\Phi}) < v_k(\mathbf{\Phi}^*)$. Thus, the scheme outlined for monodisperse suspensions also works to form concentration gradients in polydisperse suspensions of spheres with equal densities. Because of the dependence of $v_k^i(\mathbf{\Phi})$ on the concentration below the ith particle, we need to specify the composition of the artificial sublevel of packed spheres in order to calculate the velocity of spheres near the bottom. This layer should correspond to the packed bed that actually forms. However, the composition of the latter depends on the settling velocities of the various species. As an initial estimate, we set

$$\phi_j^{\max} = \phi_{\max}\phi_j^0\mathbf{1}(v_j)v_j(\mathbf{\Phi}_0)\Big/\sum_{k=1}^{K}\phi_k^0\mathbf{1}(v_k)v_k(\mathbf{\Phi}_0), \quad j = 1, \ldots, K \quad (9)$$

$$\mathbf{\Phi}_{\max} = (\phi_1^{\max}, \phi_2^{\max}, \ldots, \phi_K^{\max})^T, \quad (10)$$

and

$$\phi_{\max} = \phi_1^{\max} + \phi_2^{\max} + \cdots + \phi_K^{\max} \quad (11)$$

where $\mathbf{1}(v_k)$ is the indicator function[39]

$$\mathbf{1}(v_k) = \begin{cases} 1, & \text{if } v_k < 0, \\ 0, & \text{if } v_k \ge 0 \end{cases} \quad (12)$$

These values correspond to the concentrations of each species that would result from the initial flux if there were no allowance for trapping smaller particles by the rise of the packed bed. Thus, these values are only a first estimate of those that would occur in the region immediately above the bottom. A preliminary simulation is run long enough to establish the actual composition of the lowest part of the packed bed, that is, the part that contains the largest species. This is then taken to be the composition of the artificial layer. Using this composition, we carry out a complete simulation. For simplicity, we use a scheme in which particle velocities are not always continuous, but any jumps are very small. We use the MLB equation, but the simulation would work equally well with the Davis-Gecol,[40] Patwardhan-Tien,[41] or other models.

Procedure

Input data

The system consists of an ensemble of N particles of K species contained in a cylinder of height H and cross-sectional area

$$A = \frac{N}{H\sum_{k=1}^{K}\phi_k^0/V_k} \quad (13)$$

where $V_k = \pi d_k^3/6$ is the volume of a sphere of species k. The value of A is meaningless since we assume 1-D motion, but it is necessary to set A so that the heights and concentrations in the simulation match those in the experiment. The number of spheres of the kth species is

$$N_k = \lfloor AH\phi_k^0/V_k \rfloor \quad (14)$$

The particles are distributed in the cylinder either uniformly or randomly. For convenience, we refer to these as the deterministic and stochastic cases, though all the randomness in the latter results from the initial distribution.

Recall that each particle (at height z^i) has its own unique bin (of height h) that contains all the particles for which $0 \le z^i - z^j \le h$. The settling velocity of each particle is calculated from Eq. 8. For all particles within h of the bottom, we make use of the artificial layer. The concentrations of the species in this layer are either empirical (set on the basis of the concentrations of previous runs) or calculated from Eq. 9. The number of particles of species k in the artificial region (of height h) is

$$n_k = \lfloor Ah\phi_k^{\max}/V_k \rfloor \tag{15}$$

so the total number of spheres in the system is

$$N_t = N + N_a, \quad N_a = n_1 + n_2 + \cdots + n_K \tag{16}$$

The initial height of the active particle i of kind k is

$$z_k^i = \begin{cases} i \times H/N_k & \text{for the deterministic case} \\ \mathcal{R}(0, H) & \text{for the stochastic case} \end{cases} \tag{17}$$

where $\mathcal{R}(a, b)$ is a random number from the interval (a, b). In the artificial region, the corresponding coordinates are

$$z_k^i = \begin{cases} i \times h/n_k - h & \text{for the deterministic case} \\ \mathcal{R}(-h, 0) & \text{for the stochastic case} \end{cases} \tag{18}$$

Description of the algorithm

The particles are kept in an array that is initially sorted according to the particles' z coordinates. The time loop of the algorithm is as follows:

```
while (there are particles to settle) do
    calculate concentrations and
    velocities of active particles
    move particles
    re-sort particle array
    settle particles on packed bed
end do
```

The detailed description of particular functions is given below.

Calculate concentrations and velocities of active particles

Since we have a data structure that keeps track of the order (in terms of height), it is relatively simple to locate the lowermost particle in the bin. We start from the topmost particle N_t, and travel down until we find the first particle j with height $z^j < z^{N_t} - h$. Now we have established the bin for particle N_t. Then we take the next particle $N_t - 1$. Its bin consists of all particles from the previous bin (except for N_t), and possibly a few particles below j. So now we have to travel only from particle j down. This should be very effective, especially for regions of constant or nearly constant concentration. We proceed in this way for all active particles, from top to bottom. This algorithm can be summarized as follows

```
j_p = N_t
for k = 1 to K do c_k = 0
for i = N_t downto N_s + 1 do
    for j = j_p downto 1 while z^j > z^i - h do
    c_{k_j} = c_{k_j} + 1
    j_p = j
    φ = 0
    for k = 1 to K do
        φ_k = c_k V_k/(Ah)
        φ = φ + φ_k
    end do
    c_{k_j} = c_{k_i} - 1
    // disregard particle i in
    (i - 1)th bin
    calculate v^i from Eq. (8)
end do
```

N_s is the number of settled particles, k_i refers to the species to which particle i belongs, and c_k is the number of particles of species k in the current bin.

Move particles

The coordinates of the spheres are updated according to the equation

$$z^i = z^i + v^i \Delta t, \quad i = N_s + 1, \ldots, N_t \tag{19}$$

Resort particle array

The particle array is sorted in every time-step to facilitate easy calculation of concentrations. However, there are two problems. First, it would be inefficient to sort the whole array, since the settled particles do not move and, hence, their order does not change. On the other hand, it is not sufficient to sort only the active particles because, near the settled-active boundary z^{N_s}, the settled and active particles could have intermixed as a result of the motion process. We set Δt such that the active particles cannot travel further than h in one time-step. Below $z^{N_s} - h$, therefore, there are only settled particles that do not need resorting. Hence, we sort only the part of the particle array above the index

$$n_f = N_s - \lfloor \phi_{\max} Ah/V_K \rfloor \tag{20}$$

The other problem is that, in the sorting process, we lose information about the state of the particle (artificial, settled, or active). To solve this problem, we give the particle structure an additional field that contains information about its status. The value of this field is as follows

$$s^i = \begin{cases} 0 & \text{particle from the artificial layer} \\ 1 & \text{settled particle} \\ 2 & \text{active particle} \end{cases} \tag{21}$$

We used two sorting algorithms: quick sort and insertion sort.

Settle particles

As the particles settle into the packed bed, we encounter problems similar to those in sorting. Namely, we do not know the index of the lowest active particle. Once again we use an estimate n_f, given by Eq. 20. Then we start from particle n_f and

Table 1. Simulation Times for Different Numbers of Particles

N	T_{di} [s]	T_{dq} [s]	T_{si} [s]	T_{sq} [s]	T_{dq}/T_{di}	T_{sq}/T_{si}
2^{16}	80	105	98	131	1.31	1.34
2^{17}	165	221	205	285	1.34	1.39
2^{18}	341	463	425	614	1.36	1.44
2^{20}	1581	2034	2114	2998	1.29	1.42
2^{21}	3760	4347	5177	6551	1.16	1.27

T_{di}—time for deterministic run with insertion sort, T_{dq}—time for deterministic run with quick sort, T_{si}—time for stochastic run with insertion sort, T_{sq}—time for stochastic run with quick sort.

travel upward until the first particle for which $z^i > B$ where B is the height of the packed bed. The main settling loop is as follows

for $i = n_f$ to N_t **while** $z^i \le B$ **do**
  if $s^i = 2$ **then**
  // settle only active particles
    $N_s = N_s + 1$
    $s^i = 1$ // mark particle as settled
    $B = B + V^i/(A\phi_{\max})$
  // raise packed bed
  end if
end do

Results

Time and memory requirements

The program was written in C++ language and executed on a Pentium III processor, 800 MHz, with 128 MB RAM and 256 KB cache. Execution times of the program (in seconds) for deterministic and stochastic runs (for two sorting algorithms) are presented in Table 1. These results are for a bidisperse suspension.

The two parts that consume the most time are the calculation of concentration and sorting. We applied and tested two different sorting algorithms: quick sort, which is $\mathbb{O}(N \log_2 N)$, and insertion sort which, in the average case, is $\mathbb{O}(N^2)$ but $\mathbb{O}(N)$ in the case of already sorted (or nearly sorted) data. This is actually our case since the particle motion disturbs the order only slightly. It turns out that the program with insertion sort runs 30–40% faster than with quick sort (see columns 6 and 7 of Table 1). This advantage is slightly smaller for $N = 2^{21}$ which suggests that the quick sort might eventually give better performance for much larger N, but such values were beyond the scope of our tests.

The stochastic runs consume 30–40% more time than the deterministic case. This is probably due to the nature of the sorting algorithm, which is more effective for data that are uniformly distributed and, also, the calculation of concentrations, which works best for regions of constant concentration. The memory requirements of the program are relatively high. It requires 22 bytes per particle (which means about 44 MB for $N = 2^{21}$ particles).

Bidisperse suspensions

Using Eq. 8 with $u_{\infty_1} = -1$ cm/min, $\delta_1 = 1$, $\delta_2 = 0.8$, $d_1 = 0.1$ cm, and $\phi_{\max} = 0.66$, we simulated the sedimentation of a bidisperse suspension of 10^6 rigid spheres in a very viscous fluid. For this hypothetical example, we chose a relatively small difference in the size of the spheres so that our

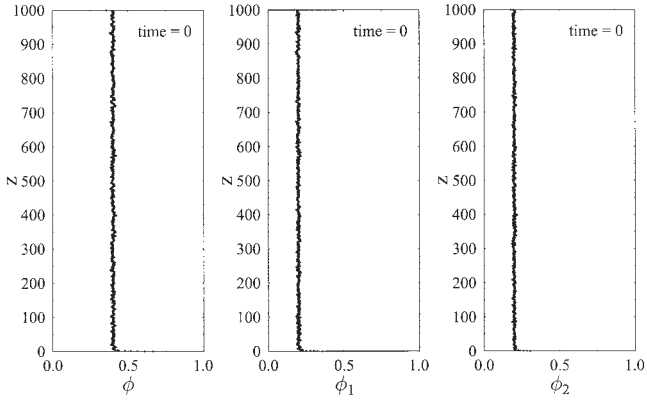

Figure 1. Initial concentration profiles in the stochastic case.

Spheres of species 1 and 2 are randomly distributed over the height of the column. $\phi_1^0 = \phi_2^0 = 0.2$, $\phi_0 = 0.4$.

results could be compared to those in the monodisperse case. Since the essential behavior of the suspension depends only on the size ratio of the two equal-density species, we defined the dimensionless variables $u^* = u/|u_{\infty_1}|$, $z^* = z/d_1$, and $t^* = t|u_{\infty_1}|/d_1$. Throughout the remainder of this section, we use these dimensionless variables, but omit the asterisks. Figure 1 shows the initial concentration profiles in the stochastic case. The slight irregularities in concentration reflect the random placement of particles.

Figure 2 shows (from the bottom up) a packed bed, a sharp change in ϕ, a concentration gradient, a region of constant concentration, and a small but sharp change to a region that contains only small spheres. Note that $\phi(z)$ is now sectionally smooth while $\phi_1(z)$ and $\phi_2(z)$ are not. However, the fluctuations in the concentrations of the two species do not increase with time. The concentration dependence (based on a region of thickness 10 whose upper boundary is z^i) controls fluctuations in $\phi_1(z)$, $\phi_2(z)$, and especially $\phi(z)$. This smoothing has already occurred by $t = 1{,}000$ (not shown). In preliminary experiments with $v_k(\mathbf{\Phi}) = 0$, $\phi \ge \phi_{\max}$, we obtained slight irregularities in the concentration of the packed bed. In the

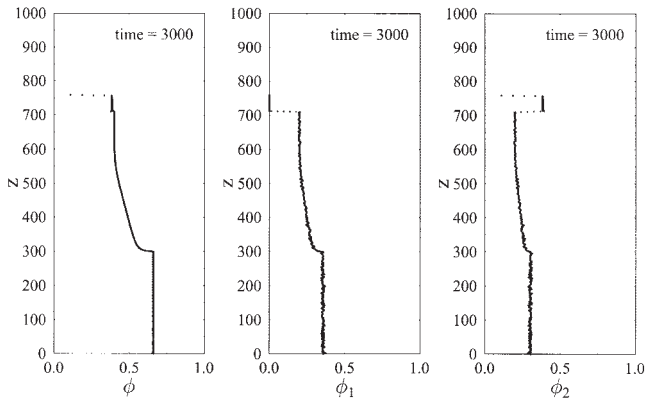

Figure 2. Concentration profiles in a bidisperse suspension with $\phi_1^0 = \phi_2^0 = 0.2$.

At $t = 3000$, the height of the packed bed is roughly 300. The region of constant concentration covers the region from about 600 to slightly above 700. The "nose" in $\phi_2(z)$ above 700 reflects the "Smith effect."

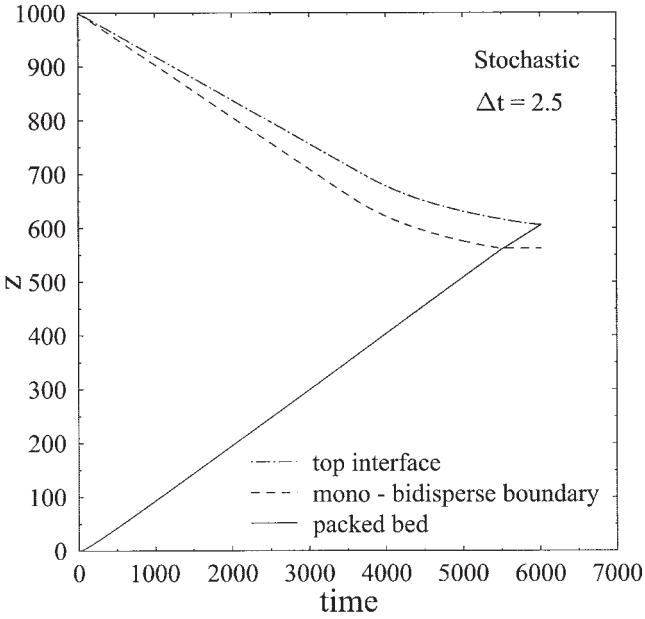

Figure 3. Settling curves for a bidisperse suspension with $\phi_1^0 = \phi_2^0 = 0.2$.

The particles were initially distributed randomly. Each curve consists of a linear section followed by gradual increase in slope (decrease in rate of fall) and an abrupt change to horizontal (zero velocity).

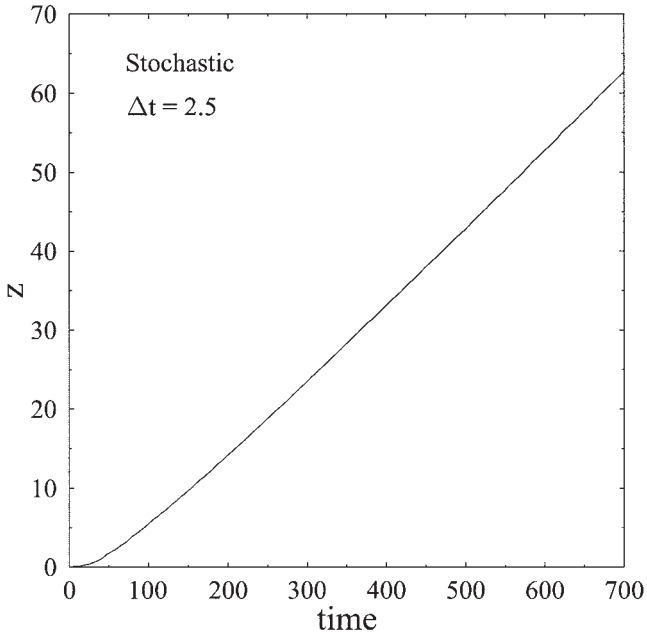

Figure 4. Initial growth of the packed bed.

The initial concentrations are $\phi_1^0 = \phi_2^0 = 0.2$, $\phi = 0.4$. The concentration of the packed bed is $\phi_{max} = 0.66$. Beyond $t = 400$, the rise is linear until all the large spheres have settled out.

work reported here, we eliminated that problem by letting spheres settle until they hit the packed bed. This duplicates the actual settling process in which spheres settle until they are supported.

Figure 3 shows the height-time curves of the mixed-small interface, the upper interface, and the rise of the packed bed. Note the slight but abrupt change in the rate of rise of the latter when the larger spheres have settled out. The first increase in ϕ at the mixed-small interface occurs at about $t = 3{,}400$, and is reflected in a very gradual decrease in its rate of fall. In the terminology of Bustos et al.,[3] both curves correspond to an MS-5 mode of sedimentation for a monodisperse suspension.[16] Proceeding upwards from $z = 0$ at $t = 3{,}000$, we traverse regions with the concentrations shown in Figure 2. At later times (not shown), the gradient reaches the mixed-small interface and subsequently induces a gradient in the zone of small spheres. The final profile (not shown) consists of a tall mixed packed bed below a short bed of small spheres.

The curve representing the rise of the packed bed is initially nonlinear, but soon attains a constant rate. Of course, it is easy to simulate the linear rise predicted by flux theory, but the simplest method (maintaining a constant rate of fall and stopping the spheres when they hit the packed bed) cannot produce a concentration gradient. In our simulation, the bin size was $h = 10$, so after the first time-step, there is a region of that height (just above the packed bed) with a concentration gradient. Since the lowest particles settle slowly into the packed bed, its rise is slow initially. Lubrication terms[2] imply that the initial rise should be slow, so the simulated results may be more accurate than the result predicted by Kynch's theory. Time-steps of 10, 5, and 2.5 were tried. Shorter time-steps lead to shorter nonlinear periods, but longer computation times. A step-size of 2.5 was adopted as a reasonable compromise. Figure 4 is an enlarged view of the initial rise with this step-size.

The concentration of the "nose" that appears in all the solids profiles for ϕ_2 can be calculated by a material balance.[42] It appears automatically in the simulations. Consider the constant-rate portion of the settling curves. We denote by ϕ_2^+ and $\phi_2^- = \phi_2^0$ the concentrations (of the small spheres) above and below the mixed-small interface. Since $v_2(\mathbf{\Phi}_0) > v_2(\phi_2^+)$, small spheres in the bidisperse suspension and those in the upper zone approach each other. In Figure 5, the dashed line (with slope $v_2(\phi_2^+)$) represents the trajectory of a sphere that is in the upper zone. This means that it crossed the mixed-small interface (which has slope $v_1(\mathbf{\Phi}_0)$) at t_1. The dotted line (with the least-negative slope $v_2(\mathbf{\Phi}_0)$) represents the path of a small sphere (in the interior of the mixed zone) that reaches the boundary at t_2. Thus

$$H_2 = [v_2(\phi_2^+) - v_1(\mathbf{\Phi}_0)](t_2 - t_1) \tag{22}$$

and

$$H_1 = [v_2(\mathbf{\Phi}_0) - v_1(\mathbf{\Phi}_0)](t_2 - t_1) \tag{23}$$

In the deterministic case, all the small spheres that were originally distributed over H_1 are now distributed over H_2. This means that $H_2\phi_2^+ = H_1\phi_2^- = H_1\phi_2^0$. It follows that

$$\phi_2^+[v_2(\phi_2^+) - v_1(\mathbf{\Phi}_0)] = \phi_2^0[v_2(\mathbf{\Phi}_0) - v_1(\mathbf{\Phi}_0)], \tag{24}$$

and, from $H_2 < H_1$, that $\phi_2^+ > \phi_2^0$. Eq. 24 is exactly the equation derived from a material balance by Smith.[42] This

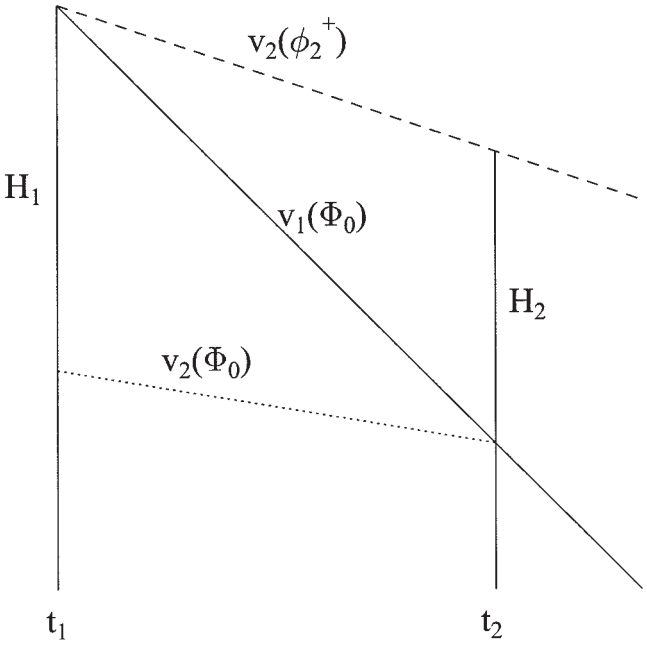

Figure 5. Converging paths of spheres in contiguous zones.

– – – Path of small sphere in upper region. — Path of mixed-small interface. · · ·Path of small sphere in lower region.

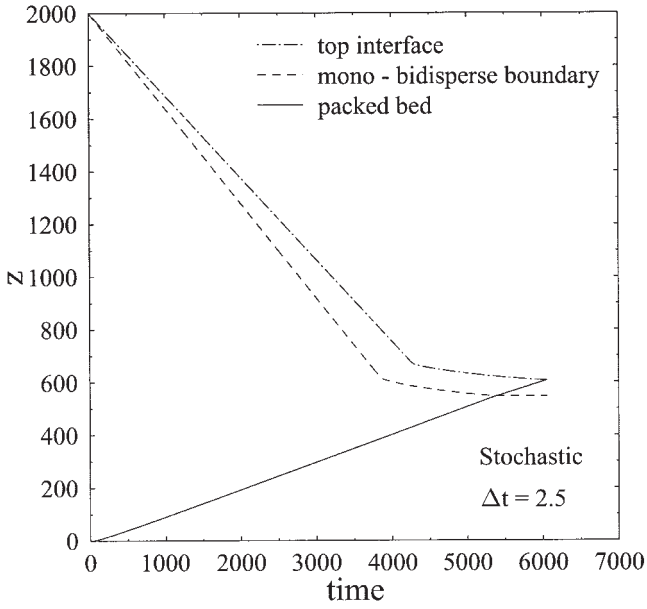

Figure 7. Settling curves for a bidisperse suspension with $\phi_1^0 = \phi_2^0 = 0.1$.

The particles were initially distributed randomly. Each curve consists of a linear section followed by an abrupt increase in slope (decrease in rate of fall), a gradual increase in slope, and an abrupt change to horizontal (zero velocity).

explains why a deterministic simulation automatically yields the correct value of ϕ_2^+. This derivation, which was suggested by Figure 3 of Tory and Pickard,[18] can be generalized to any number of species. In stochastic simulations, the velocities of individual spheres vary slightly, so the argument does not hold exactly. Nevertheless, the approximation is excellent.

Figure 6 shows the concentration profiles in a more dilute suspension. The profile for ϕ shows the packed bed, a sharp change in concentration, a gradual change, another sharp change, a region of constant concentration, and a small but abrupt change to a region that contains only small spheres. By $t = 4{,}000$, the sharp change in $\phi_1(z)$ has reached the mixed-small interface, that is, the concentration there is $\phi > \phi_0$.

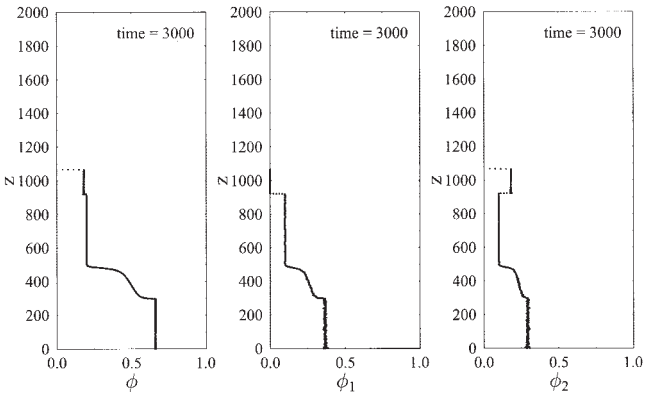

Figure 6. Concentration profiles in a bidisperse suspension with $\phi_1^0 = \phi_2^0 = 0.1$.

The two species were initially distributed randomly over $H = 2000$, leading to fluctuations in $\phi_1^0(z)$, $\phi_2^0(z)$, and $\phi_0(z)$.

Consequently, $v_2(\mathbf{\Phi}) > v_2(\mathbf{\Phi}_0)$ and ϕ_2^+ has increased sharply (not shown).

For bidisperse suspensions in which the particles were initially distributed uniformly, the concentration profiles $\phi(z)$ for $t = 1{,}000$ were indistinguishable from those in the stochastic case while those for $\phi_1(z)$ and $\phi_2(z)$ differed only in having no small fluctuations. If the fluctuations in the stochastic case were far greater and not controlled early, the concentration dependence might lead to slightly higher solids flux[22] and, hence, different profiles.

Figure 7 shows the settling curves for the bidisperse suspension whose concentration profiles were shown in Figure 6. These correspond to the mode of sedimentation labeled MS-4 for a monodisperse suspension.

Figure 8 shows the concentration profiles for a dilute bidisperse suspension. There is a sharp change in concentration from the packed bed to the initial concentration, and a small but abrupt change to a region with only small spheres. The initial concentrations persist until all the large spheres have settled out.

Figure 9 shows the settling curves for the bidisperse suspension whose concentration profiles were shown in Figure 8. These correspond to the mode of sedimentation labeled MS-1 for a monodisperse suspension. There is a small transition region in which the slope changes very rapidly from its initial value to zero. This is a consequence of the noninstantaneous change in concentration from ϕ_0 to $\phi_{\max}$. The sharp gradient (that is formed initially) remains, but does not expand.

To summarize, the bidisperse simulations produce all of the expected behavior. In particular, concentration gradients expand when they should, and do not expand when they should not. In the stochastic case, fluctuations in total concentration are quickly smoothed while the fluctuations in the concentra-

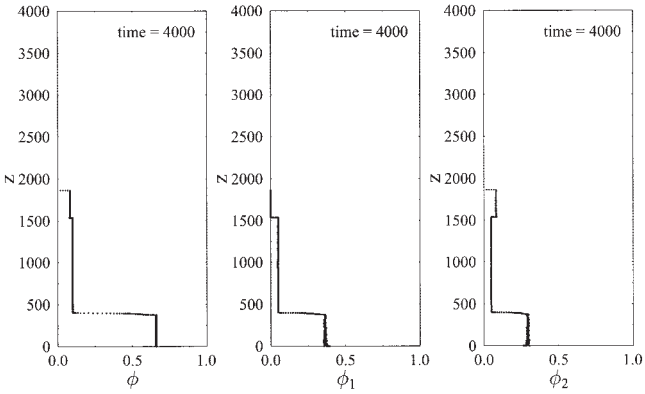

Figure 8. Concentration profiles in a bidisperse suspension with $\phi_1^0 = \phi_2^0 = 0.05$.

The two species were initially distributed randomly over $H = 4000$, leading to fluctuations in $\phi_1^0(z)$, $\phi_2^0(z)$, and $\phi_0(z)$.

tion of each species are controlled. These features are essential for future work with the Markov model.[22] Some discontinuities predicted by flux theory are replaced by abrupt changes in concentration. This is actually more realistic.

Polydisperse suspensions

Many experimenters use glass spheres that have been sieved to reduce the variation in size. For example, Shannon et al.[8] obtained a distribution of diameters that was approximately normal with mean $\mu = 66.49$ μm, and standard deviation $\sigma = 6.70$ μm. For a normal distribution, the mean surface area is $\pi(\mu^2 + \sigma^2)$ and the mean volume is $(\pi/6)\mu(\mu^2 + 3\sigma^2)$. One sphere diameter for such suspensions is often chosen as representing all the spheres in the suspension. This approximation is

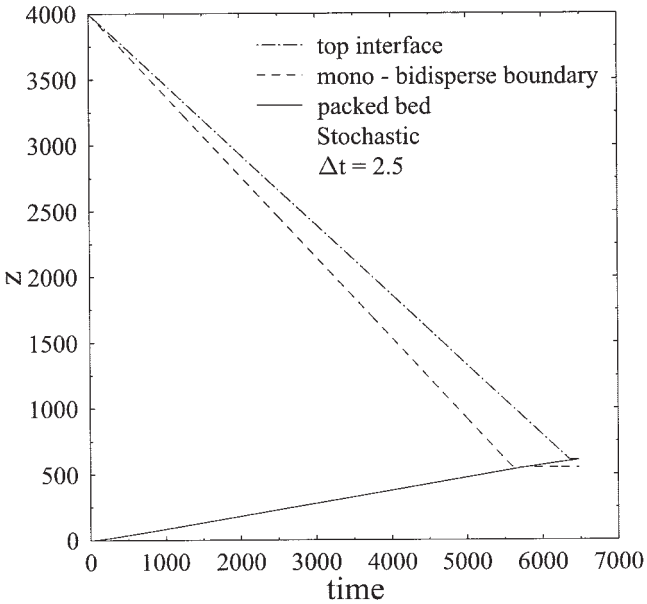

Figure 9. Settling curves for a bidisperse suspension with $\phi_1^0 = \phi_2^0 = 0.05$.

The particles were initially distributed randomly. Each curve consists of a linear section followed by an abrupt change to horizontal (zero velocity).

Table 2. Size Distribution of Spheres in Polydisperse Suspensions

Species	Diameter (μm)	Number	Volume (mm^3)	$10^4\phi_k^0$	$10^4\phi_k^0$
1	87.69	2,000	0.706	3.26	4.35
2	83.45	20,000	6.086	28.10	37.47
3	79.21	90,000	23.420	108.15	144.20
4	74.97	240,000	52.951	244.52	326.03
5	70.73	420,000	77.814	359.34	479.12
6	66.49	504,000	77.571	358.22	477.62
7	62.25	420,000	53.048	244.97	326.63
8	58.01	240,000	24.531	113.28	151.04
9	53.77	90,000	7.326	33.83	45.11
10	49.53	20,000	1.272	5.87	7.83
11	45.29	2,000	0.097	0.45	0.60
		2048000	324.822	1499.99	2000.00

based on the widespread belief that hindrance effects prevent segregation by size when ϕ_0 is sufficiently large. Though Scott and Mandersloot[43] have suggested a different representative diameter, a popular choice has been that of a sphere with the same volume-surface ratio as that of the distribution of spheres. Then d_{eff} equals 6 $\times$ (total volume/total area), which yields $d_{\text{eff}} = 67.83$ μm for the spheres used by Shannon et al.[8] Their sieving failed to remove a large number of very fine particles that constituted about 1.48% of the total volume and 2.86% of the total area. Including fines $d_{\text{eff}} = 66.94$ μm.

They measured settling rates for initial concentrations of 0.15, 0.20, 0.25, 0.30, 0.35, 0.40, 0.45, 0.50, and 0.55. They also measured the rise of the packed bed for these concentrations and for $\phi_0 = 0.05$, 0.075, and 0.10, but no upper interface could be discerned for these three values. Using a polynomial fit of initial-rate data, Shannon et al.[14] calculated the theoretical positions of the interface and packed bed from Kynch's theory,[3, 15] and compared them to experimental values.[8, 14, 44] However, the experimental values of $v(\phi_0)$ vs. ϕ_0 are also fitted very closely by a truncated Richardson-Zaki equation with $u_\infty = -3.5$ mm/s,[8] and the settling curves predicted on this basis are essentially the same.[3]

It is well known that binomial probabilities can be closely approximated by a normal distribution with $\mu = np$ and $\sigma^2 = npq = np(1 - p)$ when n is large. When $p = q$, this approximation is excellent[45] for $n \geq 10$. Conversely, a histogram (of discrete probabilities) based on a normal distribution has ordinates that closely approximate binomial probabilities with $p = q$. We took $n = 10$ and then adjusted μ, σ, and the distribution to match the mean (66.49 μm), and the standard deviation (6.70 μm) obtained by Shannon et al.[8] excluding the tail of fine particles. This implies that the resulting distribution is centered at 66.49 μm, and that the minimum separation of diameters is $(6.7/\sqrt{2.5})$ μm. Thus, as shown in Table 2, we have replaced a continuous distribution by one with 11 discrete values, each differing from the next by 4.24 μm.

The mean dia. is obviously 66.49 μm, and the standard deviation is easily calculated to be 6.70 μm, both in agreement with the experimental values of Shannon et al. The volume of each sphere of the kth species V_k, is equal to $\pi d_k^3/6$. The total volume of each species is shown in Table 2 and the last two columns give the species concentrations when $\phi_0 = 0.15$ and 0.20. The total area and volume of all the spheres in our simulations are 287.3 cm^2 and 0.3248 cm^3, respectively, the same as for a normal distribution with the same number of

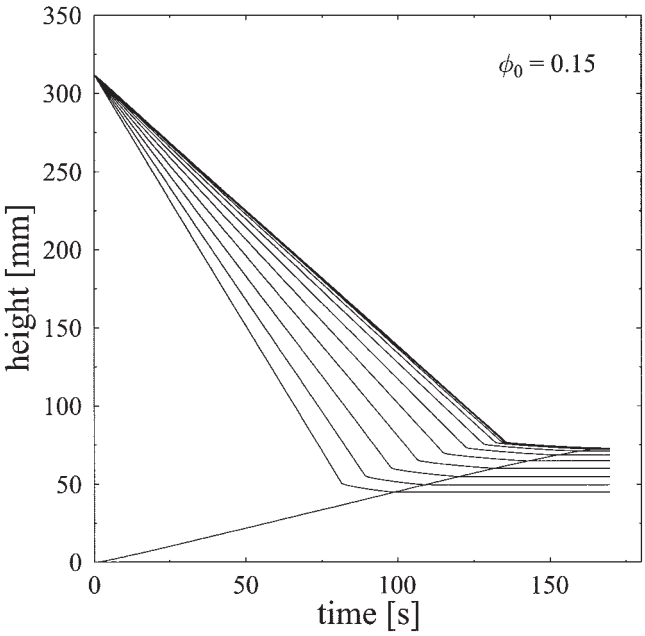

Figure 10. Settling curves for a polydisperse suspension with $\phi_0 = 0.15$.

The lines represent the position of the top sphere of each species. The lower line is the position of the top of the packed bed.

spheres. Thus, our distribution not only has the same mean and standard deviation, but also (to four significant figures) the same area, volume, and effective diameter as the normal distribution from which it was derived. This method is slightly simpler than the usual discretizing of the normal distribution, and discrete distributions (such as that in Table 2) are interesting in themselves. Approximation errors in either method are much less than the uncertainty in characterizing the distribution of diameters.[8]

Experimental height-time data for the sedimentation of these suspensions are given by Stroupe.[44] However, the first time interval is only nominally 15 s. We obtained a more accurate value of the length of this interval by extrapolating the straight-line part of the settling curve to the initial height, and the straight-line part of the curve for the packed bed to zero. The values of these first intervals need not coincide since it is unlikely that these readings were taken simultaneously.

Using the algorithm described earlier, we simulated the sedimentation of this polydisperse suspension for initial concentrations of 0.05, 0.075, 0.10, 0.15, 0.20, 0.25, 0.30, 0.35, 0.40, 0.45, 0.50, and 0.55. Shannon et al.[8] calculated that a sphere with a diameter of 66.94 μm would have a Stokes velocity of -3.92 mm/s. Then $u_{\infty 1} = -6.73$ mm/s. We used this value and adjusted the exponent n in Eq. 8 to give the best overall fit to the experimental initial-rate data. Our value, 4.95, is consistent with values in the literature, which usually range from 4.6 to 5.5.

Figure 10 shows the results for $\phi_0 = 0.15$. The lines represent the simulated positions of the top sphere of each species. Proceeding from left to right from 100 mm, there are regions containing 11, 10, . . . , 2, 1, and 0 species. The first (leftmost) region is at the original concentration $\mathbf{\Phi}_0$. The concentrations in the second region have been increased by the disappearance of species 1 (the largest size), the third by the disappearance of species 1 and 2, and so on. Thus, the concentration of species 11 increases stepwise from left to right. The uppermost part of the suspension (which reaches a maximum height of about 3 mm) contains only the smallest spheres. Nevertheless, the initial value of ϕ_{11} is so low that ϕ_{11} in this region is still small. Thus, the interface would appear to be fuzzy. Figure 9 of Shannon et al.[8] shows this very clearly. Initially, each height-time line has a constant slope. This changes abruptly, then gradually, and finally abruptly to zero. Though the period of increasing velocity is very short, this behavior corresponds to an MS-4 mode of sedimentation in a monodisperse suspension. The lower line is the position of the packed bed ($\phi_{\max} = 0.641$). After a few seconds, its rate of rise is first constant, then decreasing very gradually, and finally rapidly for a brief period at the very end. Aside from the very short initial period, eleven straight-line segments approximate the smooth curve that would be traced by the packing of spheres from a normal distribution. The experimental values of the interface (not shown) lie on or slightly above the simulated interface. The premature change in experimental velocity may reflect the difficulty in obtaining complete mixing noted by Shannon et al.[8] The experimental rise of the packed bed (not shown) coincides closely with the theoretical.

Results for $\phi_0 = 0.20$ (Figure 11) are similar to those shown in Figure 10, but the increasing rate period is much longer. The closeness of the lines (not shown) for the three smallest species implies that the interface should be much sharper than for $\phi_0 = 0.15$. After a few seconds, the packed bed first rises at a constant rate, then slows down very gradually and finally rapidly for a brief period at the very end. The experimental height-time values fall initially on a straight line, but after 75 s

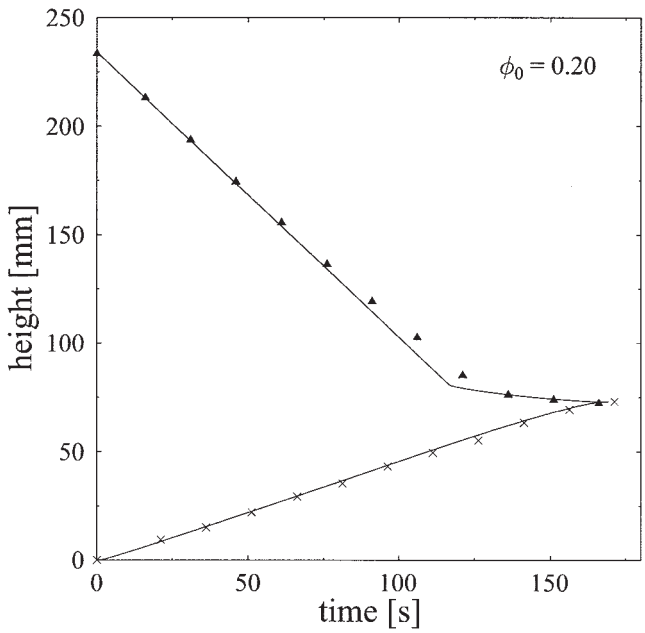

Figure 11. Settling curve for a polydisperse suspension with $\phi_0 = 0.20$.

The upper line represents the position of the top sphere. The lower line is the position of the top of the packed bed. The symbols represent the experimental values from Stroupe.[44]

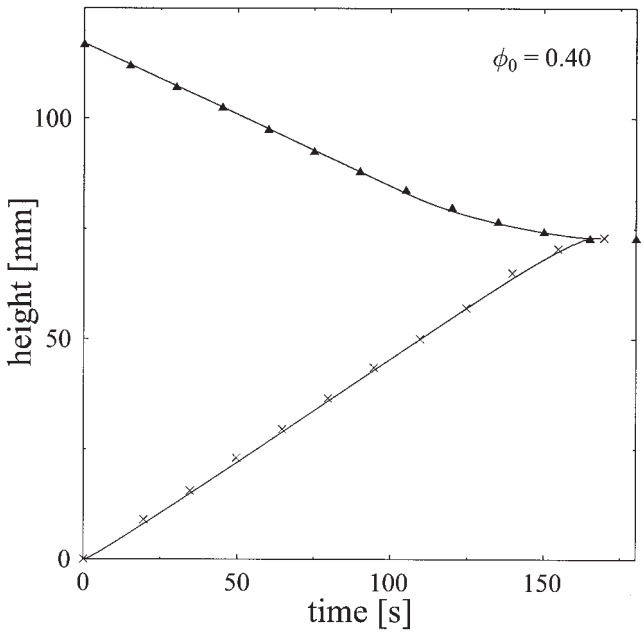

Figure 12. Settling curve for a polydisperse suspension with $\phi_0 = 0.40$.

The upper line represents the position of the top sphere. The lower line is the position of the top of the packed bed. The symbols represent the experimental values from Stroupe.[44]

they lie slightly above it. The theoretical curve for the packed bed agrees closely with the experimental points.

Curves for $\phi_0 = 0.25$ (not shown) are very similar to those for $\phi_0 = 0.20$, but the first break in slope is less pronounced. Shannon et al.[8] state that the interfaces for $\phi_0 = 0.20$ and 0.25 were also diffuse. Hydrodynamic diffusion and/or the presence of fines (not included in the theoretical analysis) could account for this difference.

Figure 12 shows the settling curve for a suspension with $\phi_0 = 0.40$. The slope of the settling curve is initially constant, then increasing gradually and finally abruptly to zero. This curve clearly corresponds to an MS-5 mode of sedimentation. The simulated upper interface fits the experimental points very well. Similarly, the theoretical and experimental values for the top of the packed bed agree very closely.

The settling curves for $\phi_0 = 0.30$ and 0.35 (not shown) were similar to those for $\phi_0 = 0.40$, but the slopes changed more rapidly after the constant-rate period. It is difficult to know whether each curve corresponds to an MS-4 mode of sedimentation in which the discontinuity is smoothed or to an MS-5. As in the more dilute suspensions, the later points lie slightly above the simulated interface, but simulated and experimental values for the top of the packed bed agree closely. Results for $\phi_0 = 0.45$ (not shown) are similar to those for $\phi_0 = 0.40$. The theoretical settling curve and the rise of the packed bed agree closely with experimental values.

Figure 13 shows that the settling curve for a suspension with $\phi_0 = 0.50$ is essentially a straight line. This corresponds to an MS-1 mode of sedimentation. There is a very short curved section as the top sphere settles into the packed bed.

The settling curve for $\phi_0 = 0.55$ (not shown) also corresponds to an MS-1 mode of sedimentation, but the slopes are greater (less negative). Once again, the theoretical and experimental values agree closely.

The settling curves for $\phi_0 = 0.05$, 0.075, and 0.10 (not shown) all correspond to the MS-1 mode of sedimentation. The initial heights are 93.5, 62.3, and 46.8 cm.[44] At these low concentrations, the influence of concentration is less important than the effect of particle diameter. Consequently, the upper lines (representing the top spheres of species 11, 10, and 9) are much more widely spread, especially for $\phi_0 = 0.05$. Experimentally, segregation was extensive, so it is not surprising that no interface could be determined. Unlike all the other comparisons of the rise of the packed bed (in which the theoretical and experimental values initially coincide), the experimental values immediately exceed the theoretical. This is consistent with the inadequate mixing noted by Shannon et al.[8] Higher concentrations near the bottom and partial segregation during mixing are sufficient to explain these results, though other phenomena, such as particle streaming[26] are not excluded.

For the initial period, there was almost perfect agreement between our theoretical calculations and the experimental results of Shannon et al.[8] for $\phi_0 \geq 0.15$. However, the "straight-line" segments of their height-time plots are actually slightly curved. After an initial period, the interface falls at a slightly lower rate as settling proceeds. From their comments on the non-constant rate for set *X* (attributed to the difficulty in obtaining complete mixing in that case), it appears that ϕ_0 may have been slightly greater in the lower regions and/or the mixing may have been insufficient to assure uniformity in the distribution of the larger spheres. Remarkably, the positions of the interface and the packed bed predicted from Kynch's theory (assuming that the behavior can be represented by a monodisperse approximation) differ only very slightly from those pre-

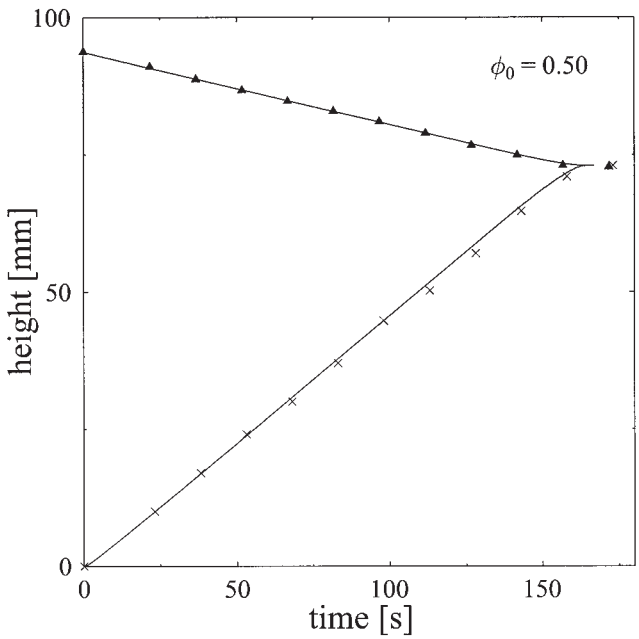

Figure 13. Settling curve for a polydisperse suspension with $\phi_0 = 0.50$.

The upper line represents the position of the top sphere. The lower line is the position of the top of the packed bed. The symbols represent the experimental values from Stroupe.[44]

dicted from the MLB model. The modes of settling are identical in both models and the rise of the packed bed is strictly linear in the first case and almost linear in the second. The difference is less than the experimental error. Of course, the MLB model predicts extensive segregation (Figure 10) while the monodisperse approximation assumes no segregation at high concentrations.

Been and Sills[46] settled flocculated suspensions of a natural soil and measured the size distribution at different heights in the compacted sediment. Despite a very wide size distribution, there was essentially no differential settling at very high concentrations. On the other hand, segregation in many polydisperse suspensions is well documented. The sharpness of the interface at higher concentrations in the experiments of Shannon et al.[8] suggests that very small spheres are moving down with the larger ones, perhaps because the former are so close to the latter that lubrication terms are important. This does not preclude some segregation by size. There are no *in situ* measurements of particle size to decide this question.

The remarkable agreement between theory and experiment[14] suggested that Kynch's theory could be applied to fairly closely sized spheres. This is true for the fall of the interface and the rise of the packed bed, but probably not for the individual species. Thus, the alternative explanation in terms of the MLB equation is of considerable interest.

Discussion

Bürger et al.[12] proved that the MLB equation predicts stability for all bidisperse suspensions in which the spheres have the same density, and conjectured that all polydisperse suspensions of this kind would be stable. This conjecture was proved by Berres et al.[37] This result ensures that three-dimensional effects are absent. Hence, our 1-D approach is justified.

Though one can sometimes follow the evolution of Φ by measuring the rise of discontinuities and using (Eq. 24) or its generalization to calculate the concentrations in the upper levels, this method is unsatisfactory for two reasons. First, a method should automatically determine the positions of discontinuities. Second, the propagation of concentration gradients in the lower region may change the concentration at the top of that region, thereby invalidating the calculation of the concentrations in the upper levels. This is clearly shown in Figures 2, 3 and 12. An important feature of the particle-based simulation is that it automatically follows the positions of discontinuities and also propagates concentration gradients when appropriate.

The principal goal of this study was to demonstrate that a particle-based approach to sedimentation is a practical alternative to sophisticated numerical methods.[11, 13] The stability of the concentration gradients and the smooth evolution of the sedimenting suspension show that the method works very well. Its simplicity and generality make it feasible to test any theoretical or empirical model against any experimental data. We plan to compare simulations with data from experiments in which the species are clearly distinguishable.

As noted by Laso,[47] simulations are easy to do and provide insights into the fundamental processes. In the ten years since his paper appeared, computing speeds have doubled six times. Simulations that then took hours now take a similar number of minutes. Simulations of nonlinear diffusion[48] that took two to three h on a 1990 workstation now take less than 30 s. In simulations of sedimentation, the number of particles has increased from one thousand[19] to two million in this study. This figure exceeds the 150 thousand to one million spheres used in the experiments of Ham and Homsy,[34] and the 1.5 million used by Nicolai et al.[49] As computing speeds increase still further, the simplicity of simulations will become more and more advantageous.

This increasing speed will facilitate the simulation of hydrodynamic diffusion in sedimentation. The particle-based approach is ideally suited to this purpose.[29] Particles can be distributed randomly (as in this study), leading to local fluctuations in concentration that play an important role in the experimental variability of particle velocities.[5, 34, 50, 51] These 3-D fluctuations are only partially captured in a 1-D model. Consequently, it is necessary to impose an additional variability in the velocity of individual particles to account for hydrodynamic diffusion. A stochastic term can be included to yield a Markov model for sedimentation[17, 18, 19, 22] that closely approximates the behavior of individual particles. The random movement of these particles produces hydrodynamic diffusion. Previous 1-D simulations using the Markov model developed local concentration inversions that grew with time.[22] In molecular diffusion, fluctuations are counterbalanced by increased outflow from regions of higher concentrations and decreased outflow from regions of lower. In simulations of sedimenting suspensions, regions of higher concentration settle more slowly. Hence, fluctuations in molecular diffusion are self-correcting,[48] while those in simulated sedimenting suspensions grow larger when fixed bins are used, especially when stochastic terms are present.[22] Thus, such simulations require that these fluctuations be smoothed. It is clear from Figures 1, 2, 6 and 8 that our scheme can do this. We deferred further modeling of stochastic processes to focus on the generation and propagation of concentration gradients, and on the control of fluctuations in concentration.

Simulations are more flexible than numerical methods. For example, we can follow the erratic path of a single large sphere through a suspension of smaller spheres and compare it to experimental results.[7, 52, 53] The number of species in a polydisperse suspension can be made as large as desired. Indeed, sampling from a normal or lognormal distribution is possible.

It is easy to apply the MLB equation to fluidization.[54, 55] The Markov model can be used to study the sharpness of the separation of two or more species. It should also be possible to study other methods of separation.[54]

Acknowledgments

We thank the reviewers for helpful comments regarding the presentation and discussion of our results.

Literature Cited

1 Happel J, Brenner H. *Low Reynolds Number Hydrodynamics.* Dordrecht: Martinus Nijhoff; 1986.
2 Kim S, Karrila SJ. *Microhydrodynamics: Principles and Selected Examples.* Boston: Butterworth-Heineman; 1991.
3 Bustos MC, Concha F, Bürger R, Tory EM. *Sedimentation and Thickening. Phenomenological Foundation and Mathematical Theory.* Dordrecht: Kluwer Academic; 1999.
4 Zeidan A, Rohani S, Bassi A, Whiting P. Review and comparison of solids settling velocity models. *Reviews in Chem Eng.* 2003;19:473–530.

5 Tory EM, Pickard DK. A three-parameter Markov model for sedimentation. *Can J Chem Eng.* 1977;55:655–665.
6 Al-Naafa MA, Selim MS. Sedimentation of monodisperse and bidisperse hard-sphere colloidal suspensions. *AIChE J.* 1992;38:1618–1630.
7 Tory EM, Kamel MT. Mean velocities in polydisperse suspensions. *Powder Technol.* 1997;93:199–207.
8 Shannon PT, Stroupe E, Tory EM. Batch and continuous thickening. Basic theory. Solids flux for rigid spheres. *Ind Eng Chem Fundam. 1963;2:203–211. Correction, ibid.* 1964;3;184.
9 Davis RH, Hassen MA. Spreading of the interface at the top of a slightly polydisperse sedimenting suspension. *J Fluid Mech. 1988;196: 107–134.*
10 Davis RH, Birdsell KH. Hindered settling of semidilute monodisperse and polydisperse suspensions. *AIChE J.* 1988;34:123–129.
11 Xue B, Sun Y. Modeling of sedimentation of polydisperse spherical beads with a broad size distribution. *Chem Eng Sci. 2003;58:1531–1543.*
12 Bürger R, Karlsen KH, Tory EM, Wendland WL. Model equations and instability regions for the sedimentation of polydisperse suspensions of spheres. *Z Angew Math Mech.* 2002;82:699–722.
13 Bürger R, Concha F, Fjelde K-K, Karlsen KH. Numerical simulation of the settling of polydisperse suspensions of spheres. *Powder Technol.* 2000;113:30–54.
14 Shannon PT, DeHaas RD, Stroupe EP, Tory EM. Batch and continuous thickening. Prediction of batch settling behavior with results for rigid spheres. *Ind Eng Chem Fundam.* 1964;3:250–260.
15 Kynch GJ. A theory of sedimentation. *Trans Faraday Soc.* 1952;48: 166–176.
16 Bürger R, Tory EM. On upper rarefaction waves in batch setting. *Powder Technol.* 2000;108:74–87.
17 Tory EM, Bargieł M, Honeycutt RL. A three-parameter Markov model for sedimentation III. A stochastic Runge-Kutta method for computing first-passage times. *Powder Technol.* 1994;80:133–146.
18 Tory EM, Pickard DK. Extensions and refinements of a Markov model for sedimentation. *J Math Anal Appl.* 1982;86:442–470.
19 Pickard DK, Tory EM. A Markov model for sedimentation: Fundamental issues and insights. In: MacNeill IB, Umphrey GJ. Advances in the statistical sciences, Vol. IV, Stochastic hydrology. Dordrecht: D. Reidell, 1987:1–25.
20 Hesse CH, Ramos E. Dynamic simulation of a stochastic model for particle sedimentation in fluids. *Appl. Math. Modelling.* 1994;18:437–445.
21 Tory EM, Ford RA. *Stochastic Simulation of Sedimentation.* In: Rahman M, Brebbia CA. Advances in Fluid Mechanics III. Southampton: WIT Press; 2000:663–672.
22 Tory EM, Ford RA. Simulation of sedimentation of bidisperse suspensions. *Int J Mineral Processing.* 2004;73:119–130.
23 Steinour HH. Rate of sedimentation. Non-flocculated suspensions of uniform spheres. *Ind Eng Chem.* 1944;36:618–624.
24 Richardson JF, Zaki WN. Sedimentation and fluidization: Part 1. *Trans Instn Chem. Engrs (London).* 1954;32:35–53.
25 Barnea E, Mizrahi JA. A generalized approach to the fluid dynamics of particulate systems, Part 1. General correlation for fluidization and sedimentation in solid multi-particle systems. *Chem Eng J.* 1973;5: 171–189.
26 Tory EM, Kamel MT, Chan Man Fong CF. Sedimentation is container-size dependent. *Powder Technol.* 1992;73:219–238.
27 Koglin B. Zum mechanismus der Sinkgeschwindigkeitserhönhung in niedrig konzentrierten Suspension. In: 27 Vorträge des 1st Europäischen Symposiums 'Partikelmesstechnik' Nürnberg, 17–19 Sept. 1975, Dechema Monographien 1589–1615, 1976: vol. 79B:235–250.
28 Pickard DK, Tory EM. A Markov model for sedimentation. *J Math Anal Appl.* 1977;60:349–369.
29 Tory EM. Stochastic sedimentation and hydrodynamic diffusion. *Chem Eng J.* 2000;80:81–89.
30 Beenakker CWJ, Mazur P. On the Smoluchowski paradox in a sedimenting suspension. *Phys Fluids.* 1985;28:767–769.
31 MacKay GDM, Mason SG. Approach of a solid sphere to a rigid plane interface. *J Colloid Sci.* 1961;16:632–635.
32 MacKay GDM, Suzuki M, Mason SG. Approach of a solid sphere to a rigid plane interface. Part 2. *J Colloid Sci.* 1963;18:103–104.
33 Brenner, H. The slow motion of a sphere through a viscous fluid towards a plane surface. *Chem Eng Sci.* 1962;17:242–251.
34 Ham JM, Homsy GM. Hindered settling and hydrodynamic dispersion in quiescent sedimenting suspensions. *Int J Multiphase Flow.* 1988;14: 533–546.
35 Masliyah JH. Hindered settling in a multiple-species particle system. *Chem Eng Sci.* 1979;34:1166–1168.
36 Lockett MJ, Bassoon KS. Sedimentation theory of binary particle mixtures. *Powder Technol.* 1979;24:1–7.
37 Berres S, Bürger R, Karlsen KH, Tory EM. Strongly degenerate parabolic-hyperbolic systems modeling polydisperse sedimentation with compression. *SIAM J Appl Math.* 2003;64:41–80.
38 Drew DA. Theory of multicomponent fluids. New York: Springer-Verlag; 1999.
39 Chung KL. *A Course in Probability Theory.* 2nd ed. New York: Academic Press; 1974.
40 Davis RH, Gecol H. Hindered settling function with no empirical parameters for polydisperse suspensions. *AIChE J.* 1994;40:570–575.
41 Patwardhan VS, Tien C, Sedimentation and fluidization in solid-liquid systems: A simple approach. *AIChE J.* 1985;31:146–149.
42 Smith TN. The sedimentation of particles having a dispersion of sizes. *Trans Instn Chem Engrs.* 1966;44:T143–T157.
43 Scott KJ, Mandersloot WGB. The mean particle size in hindered settling of multisized particles. *Powder Technol.* 1979;24:99–101.
44 Stroupe EP. *Batch Sedimentation of Rigid Spheres in a Newtonian Fluid.* Purdue University; 1962. MS Thesis.
45 Pfaffenberger RC, Patterson JH. Statistical methods for business and economics. Homewood: Richard D. Irwin; 1977.
46 Been K, Sills GC. Self-weight consolidation of soft soils: an experimental and theoretical study. *Géotechnique.* 1981;31:519–535.
47 Laso M. Stochastic dynamic approach to transport phenomena. *AIChE J.* 1994;40:1297–1311.
48 Bargieł M, Tory EM. Stochastic dynamic solution of nonlinear differential equations for transport phenomena. *AIChE J.* 1996;42:889–891.
49 Nicolai H, Herzhaft B, Hinch EJ, Oger L, Guazzelli E. Particle velocity fluctuations and hydrodynamic self-diffusion of sedimenting non-Brownian spheres. *Phys Fluids.* 1995;7:12–23.
50 Kamel MT, Tory EM, Jodrey WS. The distribution of kth nearest neighbours and its application to cluster settling in dispersions of equal spheres. *Powder Technol.* 1979;24:19–34.
51 Mucha PJ, Tee S-Y, Weitz DA, Shraiman BI. Brenner, MP. A model for velocity fluctuations in sedimentation. *J Fluid Mech.* 2004;501:71–104.
52 Verhoeven J. Prediction of batch settling behaviour. B. Chem. Eng. McMaster University, April 1963. Thesis.
53 Nicolai H, Peysson Y, Guazzelli E. Velocity fluctuations of a heavy sphere falling through a sedimenting suspension. *Phys Fluids.* 1996;8: 855–862.
54 Berres S, Bürger R, Tory EM. Applications of polydisperse sedimentation models. *Chem Eng J;* to appear.
55 Berres S, Bürger R, Tory EM. On mathematical models and numerical simulation of the fluidization of polydisperse suspensions. *Appl Math Modelling.* 2005;29:159–193.

Manuscript received May 5, 2004, revision received Dec. 29, 2004, and final revision received Feb. 4, 2005.